

Comparison between Frequency Response of Pulsating Partially Premixed and Diffusion Flame

A.M. Moustafa, M.M.Kamal, Ashraf M. Hamed, Ahmed E Hussin

Abstract: The objective of the current research is investigation of the pulsating flow effect on the size of partially premixed and diffusion flame, experimentally. The pulsation provided through a rotary ball valve in accordance with a variable speed motor arrangement increased the flame temperature and thus more heat is released. The used S-type thermocouple can measure the flame temperature at strouhal number [St] is 0 and 0.005 for the flow, the flame temperature has been measured at five planes as each plane has five radii. Fast Fourier Transform (FFT) has been used to determine the dominant frequency response of the pulsating flame temperatures. Increasing strouhal number of the mixture (LPG fuel and air) flow increases the turbulence intensity and thus the dominant frequency response of the pulsating flame increases. The dominant frequency at $St=0$ is larger than the dominant frequency at $St= 0.005$ for all the planes of the combustion chamber. Increasing strouhal number reduces the size of the pulsating partially premixed and diffusion flame by a maximum of 40 and 35 %, respectively. The pulsation process will optimize design of the burners.

Keywords: External pulsation, Oscillation flame, Inlet flame port, Partially premixed flame, Pulsation frequency, pulsejet combustor.

I. INTRODUCTION

Pulsating flames have been investigated in combustion science; the turbulent flame has been generated by the pulsation process. The pulsation process can enhance the characteristics of the turbulent flame such as; reduction of the flame length and thus optimize design of the burners. Frequency response of the turbulent flame fluctuation indicates to turbulence intensity, it can be measured by many of different techniques such as; high speed camera, infrared thermometer and thermocouple.

The researchers used high speed digital camera to investigate the characteristics of partially premixed flame. In the flame length in all the cases studied tip flickering mode of oscillations are observed at low fuel flow rates while bulk flickering mode of oscillations are observed in the flame length in all the cases studied with high fuel flow rates. At higher fuel/air flow rates and in the absence of external pulsation, shear layer instabilities set in the flame cause flame fluctuation.[1-5]

Revised Manuscript Received on October 20, 2020.

A.M. Moustafa, Ph.D. Candidate Dept., Fac. Of Eng. Ain Shams University, Egypt

M.M.Kamal, Prof. of Mechanical Power Dept., Fac. Of Eng. Ain Shams University, Egypt

Ashraf M. Hamed, Professors (Assistant) Dept., Fac. Of Eng. Ain Shams University, Egypt

Ahmed E Hussin Dept., Fac. Of Eng. Ain Shams University, Egypt

By using high speed direct/schlieren imaging and digital image processing techniques the nonlinear response of an acoustic modulated methane diffusion flame is investigated. The acoustic excitation results in changes in the observed flame oscillation frequency and flow structure evolutions in accordance to different frequency and amplitude of the excitation signals. It is found that the flame response shows a variety of expected nonlinear properties. Four types of nonlinear responses has been observed and analyzed. [6-17] Firstly, at low excitation frequencies (6–20 Hz), a bulge-merging phenomenon is observed to be responsible for the flame oscillating at half the excitation frequency, which is a common nonlinear phenomenon of frequency division. Secondly, the flow structure breaking down during the combustion process causes the doubling frequency harmonics in the frequency spectra. Thirdly, in high frequency cases, typical sub peaks, which are equal to the sum and difference of the excitation harmonics and natural flickering frequency, are observed in the nozzle region due to the interactions of buoyancy induced and acoustically driven flow structures. Finally, the excitation frequency amplitude is increased at stronger excitation perturbations, which is due to the increasing size of acoustic driven flow area. The coupling between thermal buoyancy and acoustic excitation in the upstream flame region is complex and shows typical nonlinear responses. On the one hand, the fuel/air mixing and combustion process is influenced by acoustic wave. On the other hand, the coupling between the buoyancy driven and acoustically driven flow structures affects the flame frequency consequently. The observed nonlinear frequency modes can be explained by nonlinear theory. The physical mechanisms in forming these nonlinear frequency modes have been attempted [8-25]. In the previous studies, the pulsating flow effect on characteristics of the partially premixed and diffusion flame has been investigated by using advanced equipments such as; high speed digital camera which is high accurate and more expensive. Therefore, the objective of the present research is to be experimentally investigated effect of the pulsation process on size of the partially premixed and diffusion flame by using S-type thermocouple. The measurement process of the flame temperature fluctuation has been completed at none pulsating flame ($St=0$) and pulsating flame ($St= 0.005$). The dominant frequency response of the flame which indicates to turbulence intensity has been evaluated by Fast Fourier Transform (FFT) and thus the change in size of the flame has been determined.

Comparison between Frequency Response of Pulsating Partially Premixed and Diffusion Flame

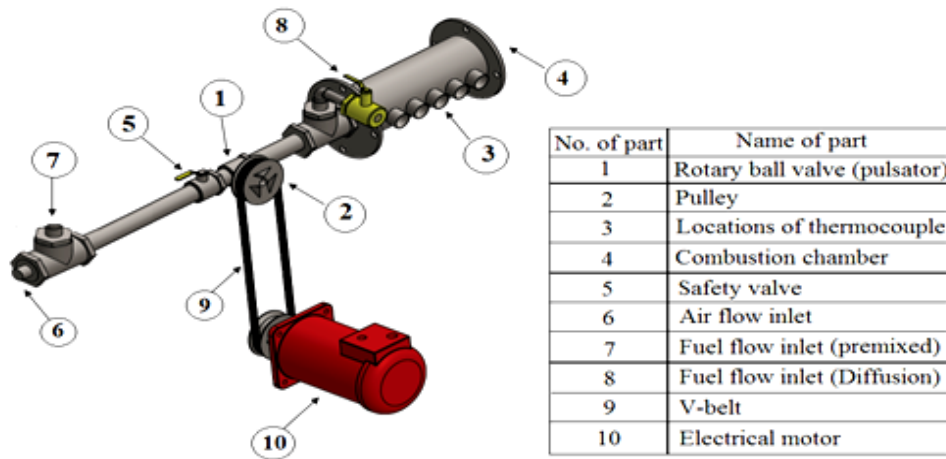


Fig.1.a. Test rig and layout of pulsating combustion system

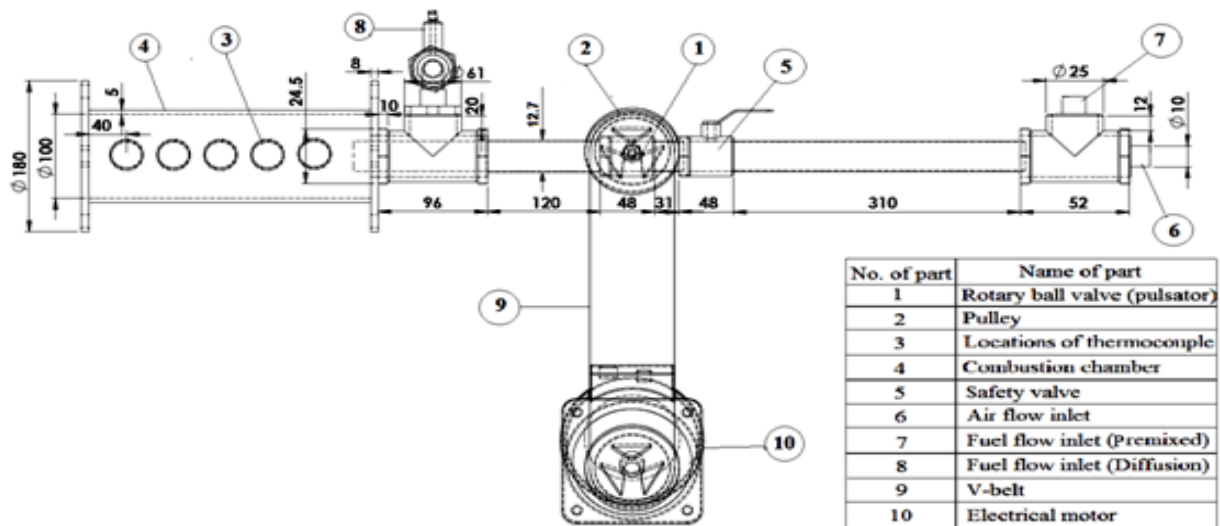


Fig.1.b. Test rig section

From Figs.1.a-b, it can be noted that pulsating process of the flow is completed through a pulley and rotary valve (pulsator) which rotate via the DC motor by V-belt. By using of the inverter, speed of the pulsating flow has been changed via the DC motor and thus there is different strouhal number of the pulsating flow. The mixture flow of fuel (LPG) and oxidizer enters the combustion chamber through diameter nozzle tip equals 12.25 mm in partially premixed case while the air flows through inner diameter nozzle tip equals 12.25 mm and fuel flows through outer diameter equals 21 mm. The flow rate of fuel and air has been measured by using four rotameters

II. TEST RIG AND EXPERIMENTAL WORK

The construction details of the test rig employed to investigate the combustion pulsating system via rotary ball valve (pulsator) are show in the following figure, (see Fig. 1.a-b).

The S-type thermocouple (Platinum/Rhodium (90%Pt, 10%Rh)), which has diameter probe equals 0.25 mm, it has been used to measure flame temperature fluctuation, instantaneously. Max 31856 module and an Arduino Uno card have been used via an Arduino circuit to display temperatures data via the computer. By using Fast Fourier Transform (FFT) excel sheet, the dominant frequency response has been determined, through input number of readings for the flame temperatures which equals 256 readings into excel sheet to output the dominant frequency response spectrum.

III. RESULTS AND DISCUSSION

In the current research, by using S- Type thermocouple, Arduino Uno circuit and Arduino program, the flame temperature fluctuation has been measured. The flame temperature fluctuation has been measured at $St= 0$ and 0.005 for the flow mixture where; $St= f.d/v$ as; $f= 0$ and 3.33 Hz, $d= 0.0127$ m and $v= 8$.



28 m/s, because the response time of the used S-type thermocouple (Δt) = 1/7 sec. and thus maximum frequency = $7/2 = 3.5$ Hz. Therefore, frequency of the pulsator = 3.33 ($St = 0.005$) \geq maximum frequency of the used thermocouple = 3.5 Hz. Accuracy of the thermocouple = ± 1.5 °C. The flame frequency has been evaluated by applying FFT (Fast Fourier Transform) and thus the dominated frequency flame is determined. The measurements has been completed at five horizontal distances (from burner inlet); 40, 70, 100, 130, 160 mm from the burner inlet. The distribution of these distances depends on studying of effect of pulsating flow on the flame length as starting of the stable flame is at 4 mm. Each distance is divided into five radii; 0, 10, 20, 30, 40 mm from center of the flame. Behind, it is completed at $A/F = 60/3 = 20$. The analysis of the results will be presented, as follows;

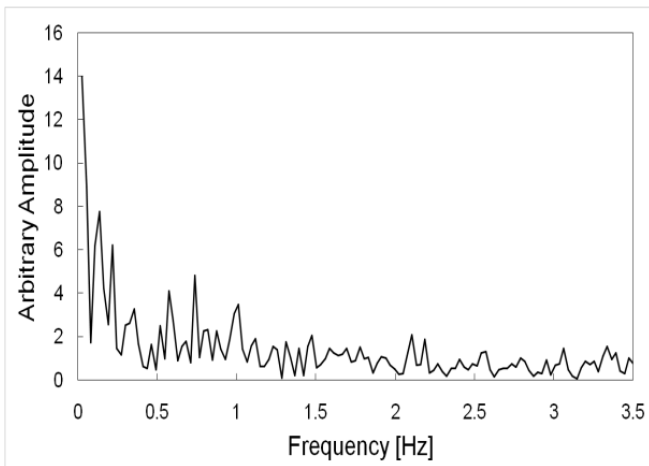


Fig. 2.a: Dominant frequency at $r = 0$ mm and $St = 0$

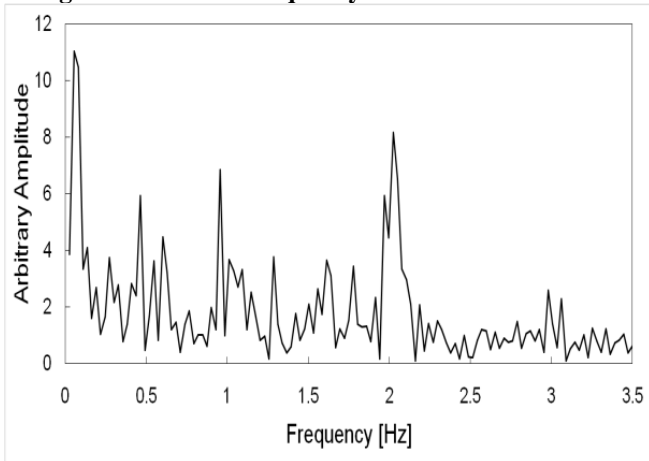


Fig. 2.b: Dominant frequency at $r = 0$ mm and $St = 0.005$

From Fig. 2.a, it can be noted that the flame frequency is dominated by the flickering due to buoyancy and the dominant frequency is 0.02 Hz, when $St = 0$ (0 rpm) and at center of the flame. In Fig. 2.b, the dominant frequency of the pulsating flame is 2.02 Hz, when $St = 0.005$ (200 rpm) and at center of the flame. In addition, from Table (1), the dominant frequencies at $St = 0.005$ are higher than the dominant frequency at $St = 0$ due to increasing strouhal number of the pulsating flow increases turbulence intensity of the flame and thus increases the temperature fluctuation and the dominant frequency.

▪ **Frequency Response at 70 mm from the Burner Inlet**

At this the plane, the dominant frequencies response will be determined at the second plane of the combustion chamber, five radii and $St = 0$ & 0.005, as follows;

A. Effect of the Pulsation on Frequency Response of the Partially Premixed Flame Temperature

Effect of the pulsating flow on frequency response of the partially premixed flame temperature fluctuation will be shown at five planes and each plane has five radii, as follows;

▪ **Frequency Response at 40 mm from the Burner Inlet**

At this the plane, the dominant frequencies response will be determined at the first plane of the combustion chamber, at five radii and strouhal number equals 0 & 0.005, as follows;

The dominant frequencies at the first plane will be shown in the following table;

Table (1): Dominant frequencies at the first plane

Radius (mm)	Dominant frequency (Hz) at $St = 0-0.005$
0	0.02-2.02
10	0.01-1.85
20	0.13-0.41
30	0.01-0.27
40	0.109-0.11

At center of the flame, the dominant frequencies will be illustrated in the following figure; The dominant frequencies at the second plane will be shown in the following table;

Table (2): Dominant frequencies at the second plane

Radius (mm)	Dominant frequency (Hz) at $St = 0-0.005$
0	0.109-0.11
10	0.1-0.3
20	0.08-0.19
30	0.07-0.16
40	0.05-0.11

From Table (2), it can be noted that the dominant flame frequencies at $St = 0.005$ are still higher than the dominant flame frequencies at $St = 0$ such as the trend of the dominant frequencies at the second plane.

▪ **Frequency Response at 100 mm from the Burner Inlet**

At this the plane, the frequency response will be determined at the third plane of the combustion chamber, five radii and $St = 0$ & 0.005, as follows;

The dominant frequencies at the third plane will be shown in the following table;

Table (3): Dominant frequencies at the third plane

Radius (mm)	Dominant frequency (Hz) at $St = 0-0.005$
0	0.109-1.94
10	0.1-0.41
20	0.1-0.27
30	0.1-0.22
40	0.1-0.27

From table (3), in addition, it can be noted that the trend of the dominant flame frequencies at $St = 0.005$ is higher than the dominant flame frequencies at $St = 0$.



Comparison between Frequency Response of Pulsating Partially Premixed and Diffusion Flame

Frequency Response at 130 mm from the Burner Inlet

At this the plane, the frequency response will be determined at the fourth plane of the combustion chamber, five radii and $St=0$ & 0.005 , as follows;

The dominant frequencies at the fourth plane will be shown in the following table;

Table (4): Dominant frequencies at the fourth plane

Radius (mm)	Dominant frequency (Hz) at $St=0-0.005$
0	0.13-2.1
10	0.05-1.05
20	0.08-0.72
30	0.05-0.4
40	0.05-0.29

From Table (4), also, it can be noted that at the current plane, the trend of the dominant frequencies is the same trend of the dominant frequencies at the first, second and third plane.

Frequency Response at 160 mm from the Burner Inlet

At this the plane, frequency response will be determined at the fifth plane of the combustion chamber, five radii and $St=0$ & 0.005 , as follows;

The dominant frequencies at the fifth plane will be shown in the following table;

Table (5): Dominant frequencies at the fifth plane

Radius (mm)	Dominant frequency (Hz) at $St=0-0.005$
0	0.109-1.49
10	0.1-0.85
20	0.02-0.21
30	0.02-0.19
40	0.02-0.08

From Table (5), also, it can be noted that the dominant frequencies at $St=0.005$ is higher than the dominant frequency at $St=0$ such as the previous planes.

B. Effect of the Pulsation on Frequency Response of the Diffusion Flame Temperature

Effect of the pulsating flow on frequency response of the diffusion flame temperature fluctuation will be shown at five planes and radii, as follows;

Frequency Response at 40 mm from the Burner Inlet

In this the part, frequency response will be determined at the first plane of the combustion chamber, at five radii and strouhal number equals 0 & 0.005 , as follows;

The dominant frequencies at the first plane will be shown in the following table;

Table (6): Dominant frequencies at the first plane

Radius (mm)	Dominant frequency (Hz) at $St=0-0.005$
0	0.03-0.16
10	0.05-0.11
20	0.27-0.43
30	0.08-0.44
40	0.14-0.19

From Table (6), it can be noted that the flame frequency is dominated by the flickering due to buoyancy and the

dominant frequency is 0.03 Hz, when $St=0$ (0 rpm) and at center of the flame. In addition, the dominant frequency of the pulsating flame is 0.16 Hz, when $St=0.005$ (200 rpm) and at center of the flame. The dominant frequencies at $St=0.005$ is higher than the dominant frequencies at $St=0$ due to increasing strouhal number of the pulsating flow increases turbulence intensity of the flame and thus increases the temperature fluctuation and the dominant frequency.

Frequency Response at 70 mm from the Burner Inlet

At this the plane, frequency response will be determined at the second plane of the combustion chamber, five radii and $St=0$ & 0.005 , as follows;

The dominant frequencies at the second plane will be shown in the following table;

Table (7): Dominant frequencies at the second plane

Radius (mm)	Dominant frequency (Hz) at $St=0-0.005$
0	0.08-0.3
10	0.05-0.4
20	0.11-0.52
30	0.11-0.44
40	0.03-0.46

From Table (7), in addition, it can be noted that the dominant flame frequencies at $St=0.005$ is still higher than the dominant flame frequencies at $St=0$.

Frequency Response at 100 mm from the Burner Inlet

In this the part, the frequency response will be determined at the third plane of the combustion chamber, five radii and $St=0$ & 0.005 , as follows;

The dominant frequencies at the third plane will be shown in the following table;

Table (8): Dominant frequencies at the third plane

Radius (mm)	Dominant frequency (Hz) at $St=0-0.005$
0	0.19-0.3
10	0.05-0.11
20	0.027-0.27
30	0.14-0.49
40	0.05-0.16

From Table (8), also, at the current plane, it can be noted that trends of the dominant flame frequencies data at $St=0$ and 0.005 are such as trends of the dominant flame frequencies data at the previous planes.

Frequency Response at 130 mm from the Burner Inlet

At this the plane, the frequency response will be determined at the fourth plane of the combustion chamber, five radii and $St=0$ & 0.005 , as follows;

The dominant frequencies at the fourth plane will be shown in the following table;



Table (9): Dominant frequencies at the fourth plane

Radius (mm)	Dominant frequency (Hz) at St= 0-0.005
0	0.027-0.25
10	0.19-0.98
20	0.08-0.38
30	0.027-0.19
40	0.11-0.24

From Table (9), In addition, it can be noted that the dominant frequencies at St= 0.005 is still higher than the dominant frequencies at St= 0 such as the previous planes.

Frequency Response at 130 mm from the Burner Inlet

At this the plane, frequency response will be determined at the fifth plane of the combustion chamber, five radii and St= 0 & 0.005, as follows;

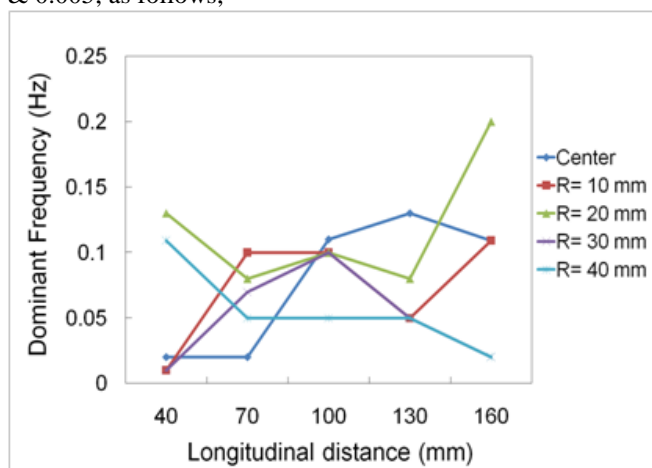


Fig.3.a. Distributions of dominant frequencies at the non-pulsating flame (Partially premixed case)

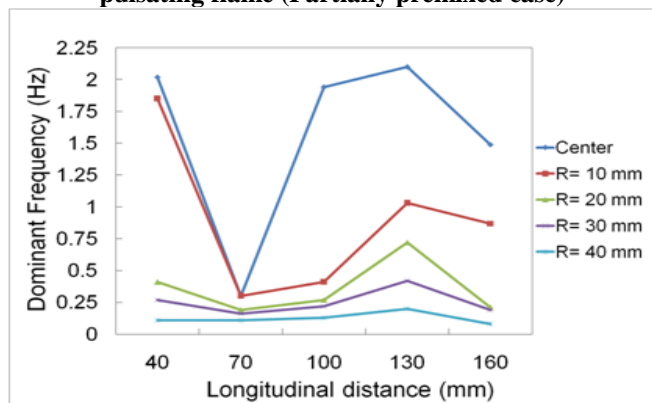


Fig.3.b. Distributions of dominant frequencies at the pulsating flame (Partially premixed case)

The dominant frequencies at the fifth plane will be shown in the following table;

Table (10): Dominant frequencies at the fifth plane

Radius (mm)	Dominant frequency (Hz) at St= 0-0.005
0	0.027-0.08
10	0.027- 0.16
20	0.055- 0.22
30	0.08- 0.1
40	0.027- 0.22

From Table (10), also, it can be noted that the dominant frequencies at St= 0.005 is higher than the dominant frequencies at St= 0.

C. Distributions of the Dominant Frequencies in the Axial Direction of the Combustion Chamber

In this the part, distributions of the dominant frequencies in the axial direction of the combustion chamber at partially premixed and diffusion flame cases will be shown as follows;

Dominant Frequencies at the Partially Premixed Flame Case

Distributions of dominant frequencies at the partially premixed flame will be shown in the following tables;

Table (11): Distributions of dominant frequencies at the non- pulsating flame (St=0)

Planes (mm) \ Radii (mm)	40	70	100	130	160
0	0.02	0.109	0.19	0.027	0.027
10	0.01	0.1	0.05	0.19	0.027
20	0.13	0.08	0.027	0.08	0.055
30	0.01	0.07	0.14	0.027	0.08
40	0.109	0.05	0.05	0.11	0.027

In addition, distributions of dominant frequencies at the pulsating flame will be shown in the following table;

Table (12): Distributions of dominant frequencies at the non-pulsating flame (St=0.005)

Planes (mm) \ Radii (mm)	40	70	100	130	160
0	2.02	0.11	1.94	2.1	1.49
10	1.85	0.3	0.41	1.05	0.85
20	0.41	0.19	0.27	0.72	0.21
30	0.27	0.16	0.22	0.4	0.19
40	0.11	0.11	0.27	0.29	0.08

The distributions of the dominant frequencies will be show in the following figures; From Fig. 3.a, it can be seen that the maximum dominant frequencies are 0.109 Hz at St= 0 and 160 mm from the burner inlet at center of the flame, while in Fig. 3.b, the maximum dominant frequency is 1.9 and 2.1 Hz at St= 0.005 and 100, 130 mm from the burner inlet and center of the flame. In Fig. 3.a, the maximum dominant frequency is 0.1 Hz at St= 0, 70 mm from the burner inlet and r= 10 mm, while in Fig. 3.b, the maximum dominant frequency is 1.85 Hz at St= 0.005, 40 mm from the burner inlet. In Fig. 3.a, the maximum dominant frequency is 0.2 at St= 0, 160 mm from the burner inlet and r= 20 mm, while in Fig. 3.b, the maximum dominant frequency is 0.72 Hz at St= 0.005 and 130 mm from the burner inlet. In Fig. 3.a, the maximum dominant frequency is 0.1 Hz at St= 0, 130 mm from the burner inlet and r= 30 mm, while in Fig. 3.b, the maximum dominant frequency is 0.42 Hz at St= 0.005 and 100 mm from the burner inlet



Comparison between Frequency Response of Pulsating Partially Premixed and Diffusion Flame

In Fig. 3.a, the maximum dominant frequency is 0.109 Hz at $St = 0$, 100 mm from the burner inlet and $r = 40$ mm, while in Fig. 3.b, the maximum dominant frequency is 0.2 at $St = 0.005$ and 100 mm from the burner inlet.

It is noted that at the pulsating condition, the density of the vortices and eddies are more in the regions which nearest to burner inlet due to the kinetic energy of the flow is high. Therefore, the maximum dominant frequencies occur at the regions that locate nearest to the burner inlet and thus the flame is shorter. Design of the burner is smaller in the length. [13, 17, 23]. This will be shown in the following figures

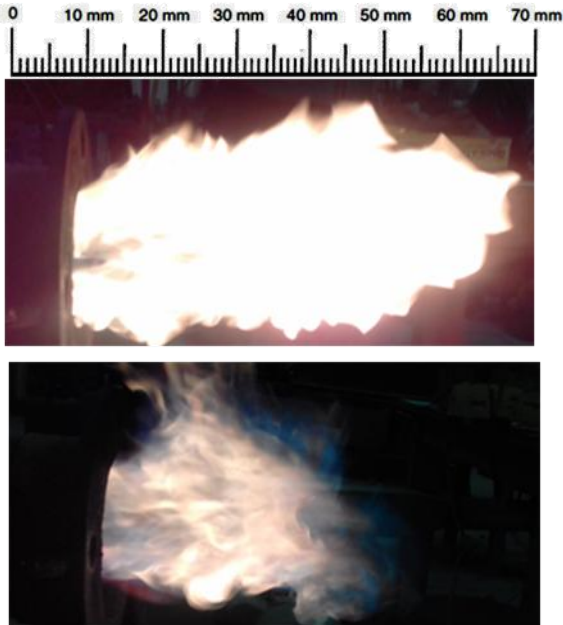


Fig. 4: length with and without pulsation

From Fig. 4, it can be seen that the pulsating flow reduces the flame length by 40% since the pulsation process causes shearing between the flame layers and thus generates vortices and eddies. The pulsation process shrinks the flame length.

▪ Dominant Frequencies at Diffusion Flame Case

Distributions of the dominant frequencies at the diffusion flame will be shown in the following tables;

Table (13): Distributions of dominant frequencies at the non- pulsating flame ($St=0$)

Planes (mm) \ Radii (mm)	40	70	100	130	160
0	0.03	0.08	0.19	0.027	0.027
10	0.05	0.05	0.05	0.19	0.027
20	0.027	0.11	0.027	0.08	0.055
30	0.08	0.11	0.14	0.027	0.08
40	0.136	0.03	0.05	0.11	0.027

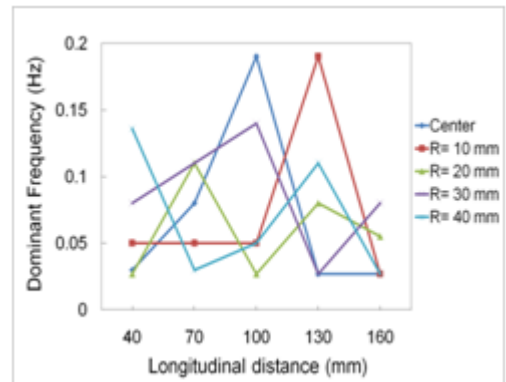


Fig.5.a. Distributions of dominant frequencies at the non-pulsating flame(Diffusion case)

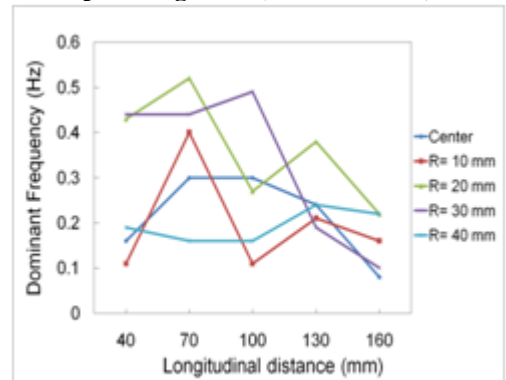


Fig.5.b. Distributions of dominant frequencies at the pulsating flame(Diffusion case)

From Fig. 5.a, it can be seen that the maximum dominant frequency is 0.19 Hz at $St = 0$ and 100 mm from the burner inlet at center of the flame, while in Fig. 5.b, the maximum dominant frequency is 0.3 Hz at $St = 0$ and 70, 100 mm from the burner inlet and center of the flame. In Fig. 5.a, the maximum dominant frequency is 0.19 Hz at $St = 0$, 130 mm from the burner inlet and $r = 10$ mm, while in Fig. 5.b, the maximum dominant frequency is 0.21 Hz at $St = 0.005$, 130 mm from the burner inlet and $r = 10$ mm. In Fig. 5.a, the maximum dominant frequency is 0.11 at $St = 0$, 70 mm from the burner inlet and $r = 20$ mm, while in Fig. 5.b, the maximum dominant frequency is 0.52 Hz at $St = 0.005$, 70 mm from the burner inlet and $r = 20$ mm. In Fig. 5.b, the maximum dominant frequency is 0.14 Hz at $St = 0$, 100 mm from the burner inlet and $r = 30$ mm, while in Fig. 5.b, the maximum dominant frequency is 0.49 Hz at $St = 0.005$ and 100 mm from the burner inlet. In Fig. 5.a, the maximum dominant frequency is 0.13 Hz at $St = 0$, 100 mm from the burner inlet and $r = 40$ mm, while in Fig. 5.b, the maximum dominant frequency is 0.46 at $St = 0.005$ and 100 mm from the burner inlet.

In addition, distributions of dominant frequencies at the pulsating flame will be shown in the following table;

Table (14): Distributions of dominant frequencies at the pulsating flame ($St = 0.005$)

Planes (mm) \ Radii (mm)	40	70	100	130	160
0	0.16	0.3	0.3	0.24	0.08
10	0.11	0.4	0.11	0.21	0.16



20	0.43	0.52	0.27	0.38	0.22
30	0.44	0.44	0.49	0.19	0.11
40	0.19	0.46	0.16	0.24	0.22

The distributions of the dominant frequencies will be shown in the following figures; In addition, It is noted that at the pulsating condition, the density of the vortices and eddies are more in the regions which nearest to burner inlet due to the kinetic energy of the flow is high. Therefore, the maximum dominant frequencies occur at the regions that locate nearest to the burner inlet and thus the flame is shorter. Design of the burner is smaller in the length. [13, 17, 23]. This will be shown in the following figures;



Fig.6. Flame length with and without pulsation

From Fig. 6, it can be seen that the pulsating flow reduces the flame length by 35% since the pulsation process causes shearing between the flame layers and thus generates vortices and eddies. The pulsation process shrinks the flame length. In partially premixed case the length of flame is shorter than the length of flame in diffusion case due to in the partially premixed case, the mixture (fuel and air) has been pulsated and thus the vortices and eddies are more, while in diffusion case the air flow has been pulsated only and thus the vortices and eddies are less.

IV. CONCLUSIONS

The obtained results showed that:

- Pulsation of the flow mixture (fuel LPG and air) generates eddies and vortices and thus turbulent flame occurred in the partially premixed and diffusion case.
- Increasing strouhal number of the flow increases the frequency response of the pulsating flame in the partially premixed and diffusion case.
- Increasing strouhal number of the pulsating flow shrinks the pulsating flame length.
- Length of the partially premixed flame case is shorter than length of the flame diffusion case.

REFERENCES

1. Plavnik, Z.Z., Severyanin, V.S., Matta, L.M. and Feingold, V.L., 2001. Pulse combustion system and method. U.S. Patent 6,210,149.
2. Plavnik, G., 2006, May. Pulse combustion technology. In 14th Annual North American Waste-to-Energy Conference (pp. 143-148). American Society of Mechanical Engineers Digital Collection.
3. Keller, J.O. and Hongo, I., 1990. Pulse combustion: The mechanisms of NOx production. *Combustion and Flame*, 80(3-4), pp.219-237.
4. Poppe, C., Sivasegaram, S. and Whitelaw, J.H., 1998. Control of NOx emissions in confined flames by oscillations. *Combustion and Flame*, 113(1-2), pp.13-26.
5. Dec, J.E. and Keller, J.O., 1989. Pulse combustor tail-pipe heat-transfer dependence on frequency, amplitude, and mean flow rate.
6. Boulanger, J., 2010. Laminar round jet diffusion flame buoyant instabilities: Study on the disappearance of varicose structures at ultra-low Froude number. *Combustion and flame*, 157(4), pp.757-768.
7. Biswas, K., Zheng, Y., Kim, C.H. and Gore, J., 2007. Stochastic time series analysis of pulsating buoyant pool fires. *Proceedings of the Combustion Institute*, 31(2), pp.2581-2588.
8. Kartheekyan, S. and Chakravarthy, S.R., 2006. An experimental investigation of an acoustically excited laminar premixed flame. *Combustion and flame*, 146(3), pp.513-529.
9. Fujisawa, N., Abe, T., Yamagata, T. and Tomidokoro, H., 2014. Flickering characteristics and temperature field of premixed methane/air flame under the influence of co-flow. *Energy conversion and management*, 78, pp.374-385.
10. Kartheekyan, S. and Chakravarthy, S.R., 2006. An experimental investigation of an acoustically excited laminar premixed flame. *Combustion and flame*, 146(3), pp.513-529.
11. Berg, I.A., Khudyakov, P.Y. and Oschepkova, V.Y., 2016. Automation of analytic complex for the investigation of pulsating combustion. *Fundamental research*, 6, pp.24-28.
12. Berg, I.A., Porshnev, S.V., Oschepkova, V.Y. and Medvedev, A.N., 2017, June. Frequency-domain analysis for pulsating combustion of gaseous fuel. In *AIP Conference Proceedings (Vol. 1836, No. 1, p. 020036)*. AIP Publishing LLC.
13. Sawarkar, P., Sundararajan, T. and Srinivasan, K., 2017. Effects of externally applied pulsations on LPG flames at low and high fuel flow rates. *Applied Thermal Engineering*, 111, pp.1664-1673.
14. Nicoli, C., Haldenwang, P. and Suard, S., 2005. Analysis of pulsating spray flames propagating in lean two-phase mixtures with unity Lewis number. *Combustion and flame*, 143(3), pp.299-312.
15. Hamins, A., Yang, J.C. and Kashiwagi, T., 1992, January. An experimental investigation of the pulsation frequency of flames. In *Symposium (international) on combustion (Vol. 24, No. 1, pp. 1695-1702)*. Elsevier.
16. Yilmaz, H., Cam, O. and Yilmaz, I., 2020. Experimental investigation of flame instability in a premixed combustor. *Fuel*, 262, p.116594.
17. Coats, C.M., Chang, Z. and Williams, P.D., 2010. Excitation of thermoacoustic oscillations by small premixed flames. *Combustion and flame*, 157(6), pp.1037-1051.
18. Yang, F. and Kong, W., 2015. Pulsating instability in H₂-air partially premixed flames. *Proceedings of the Combustion Institute*, 35(1), pp.1057-1064.
19. McQuay, M.Q., Dubey, R.K. and Carvalho Jr, J.A., 2000. The effect of acoustic mode on time-resolved temperature measurements in a Rijke-tube pulse combustor. *Fuel*, 79(13), pp.1645-1655.
20. Kilicarslan, A., 2005. Frequency evaluation of a gas-fired pulse combustor. *International journal of energy research*, 29(5), pp.439-454.
21. Saitoh, T. and Otsuka, Y., 1976. Unsteady behavior of diffusion flames and premixed flames for counter flow geometry. *Combustion Science and Technology*, 12(4-6), pp.135-146.
22. Searby, G., 1992. Acoustic instability in premixed flames. *Combustion science and technology*, 81(4-6), pp.221-23.
23. Wang, Q., Huang, H.W., Tang, H.J., Zhu, M. and Zhang, Y., 2013. Nonlinear response of buoyant diffusion flame under acoustic excitation. *Fuel*, 103, pp.364-372.
24. Balachandran, R., Ayoola, B.O., Kaminski, C.F., Dowling, A.P. and Mastorakos, E., 2005. Experimental investigation of the nonlinear response of turbulent premixed flames to imposed inlet velocity oscillations. *Combustion and Flame*, 143(1-2), pp.37-55.

Comparison between Frequency Response of Pulsating Partially Premixed and Diffusion Flame

25. McQuay, M.Q., Dubey, R.K. and Carvalho Jr, J.A., 2000. The effect of acoustic mode on time-resolved temperature measurements in a Rijke-tube pulse combustor. *Fuel*, 79(13), pp.1645-1655

AUTHORS PROFILE



Ahmed Mohamed Moustafa borned in Cairo, Egypt. Ahmed graduated from the Faculty of Engineering, Ain Shams University in 2009, Cairo, Egypt, He studied in Mechanical Engineering department. He concerns with combustion Engineering and internal combustion engine.



Mohmoud Mohamed Kamal borned in Cairo, Egypt. Mahmoud graduated from the Faculty of Engineering, Ain shams University in 1998, Cairo, Egypt. He studied in Mechanical power engineering department. He is current a Lecturer at the department of Mechanical Power Engineering since 2005. He concerns with combustion engineering, internal combustion engine, thermo fluid, heat transfer, fluid mechanics, and turbo machine.



Ashraf Mostafa Hamed borned in Cairo, Egypt. Ashraf graduated from the Faculty of Engineering, Ain shams University in 2003. He is current a Lecturer at the department of Mechanical Power Engineering since 2013. He concerns with Turbomachinery, Wind Energy, Fluid Dynamics, Combustion and Computational Fluid Dynamics.



Ahmed Mohamed Hussein borned in Cairo, Egypt. Ahmed from the Faculty of Engineering, Ain shams University in 2000. He is current a Lecturer at the department of Mechanical Power Engineering since 2012. He concerns with Fluid Mechanics Computational Fluid Dynamics, Engineering Thermodynamics, Turbulence, Energy Engineering, Heat Exchangers, Experimental Fluid Mechanics, Applied Thermodynamics, Heat Transfer Convection.